

Short communication

YSZ-based SOFC with modified electrode/electrolyte interfaces for operating at temperature lower than 650 °C

Mingfei Liu, Dehua Dong, Ranran Peng, Jianfeng Gao, Juan Diwu,
Xingqin Liu, Guangyao Meng*

*Laboratory for Solid State Chemistry & Inorganic Membranes, Department of Materials Science and Engineering,
University of Science and Technology of China, Hefei 230026, Anhui, China*

Received 23 January 2008; accepted 26 January 2008

Available online 7 February 2008

Abstract

A NiO/Yttrium-stabilized zirconia (YSZ) transition layer and/or a SDC function layer were introduced into the anode/electrolyte and/or electrolyte/cathode interface to decrease the activation polarization resulted from the mass transfer at electrode/electrolyte interface. With a NiO/YSZ transition layer, the activation polarization simulated from I - V curves drops from 4.42 to 2.42 Ω cm² at 600 °C, about 45% less than that of cell I; with additional SDC function layer, no activation polarization is obviously observed. The cell performance was also remarkably improved with the introduction of both the transition layer and the SDC function layer. Peak power densities of 187 and 443 mW cm⁻² at 600 and 650 °C, respectively, were achieved for a single cell with both a transition layer and a function layer, with an increment of 87% and 95% compared to that of the cell without any structural improvement, and about 30% and 25% compared to that of the cell with only anode transition layer. The study by ac impedance spectroscopy technique also indicated that the interfacial polarization resistance, the main source of cell resistance, could be effectively reduced by interface improvement.

© 2008 Elsevier B.V. All rights reserved.

Keywords: Yttrium-stabilized zirconia (YSZ); Solid oxide fuel cells (SOFCs); Interface modification; Microstructure; Activation polarization

1. Introduction

Solid oxide fuel cells (SOFCs) have been extensively studied as a great energy conversion device with high electrical efficiency, low emission and high tolerance to various fuels [1,2]. Traditional SOFCs adopt yttrium-stabilized zirconia (YSZ) as electrolyte, and usually operate at 800–1000 °C to achieve desirable cell performance due to the low conductivity of YSZ. In the past 10 years, most efforts in SOFCs development have been aimed at lowering the operating temperatures down to 600–800 °C to avoid obstacles encountered by traditional SOFCs, such as the lack of sealing materials, the volatility of Cr element in ceramic interconnects, and the obvious interaction among the component materials. There have been two major approaches to reduce cell resistance

at reduced temperatures: searching for new electrolyte materials with higher ionic conductivity, and/or reducing the thickness of electrolyte. Doped ceria (DCO) and doped lanthanum gallate exhibit much higher ionic conductivity than YSZ at intermediate temperatures (>500 °C), and are regarded as candidate electrolyte. But these two materials cannot completely replace YSZ electrolyte in SOFC commercialization because of their notable shortcomings, such as low mechanical strength and chemical stability of doped ceria, and poor chemical compatibility of lanthanum gallate with NiO anode.

Various techniques, such as suspension spray [3], tape casting [4], screen-printing [5], sol-gel method [6], dip-coating [7], spin-coating [8] and spin smoothing method [9], have been developed to deposit thin electrolyte film around 10 μ m and even less on porous anode support to reduce the bulk resistance of cells. And the power densities of such cells are usually above 500 mW cm⁻² and even close to 2 W cm⁻² at temperature lower than 800 °C, depending on the electrolyte material and thickness, as well as the cell configuration and fabrication details

* Corresponding author. Tel.: +86 551 3603234; fax: +86 551 3607627.

E-mail addresses: mfliu@mail.ustc.edu.cn (M. Liu), mgym@ustc.edu.cn (G. Meng).

[10,11]. The well development of fabrication techniques makes YSZ still the preferred electrolyte material for SOFC, because of its unique characteristics, such as pure ionic conductivity over a wide range of ambient conditions, high chemical and thermal stability and excellent mechanical properties.

However, the cell performance with YSZ electrolyte is still too low for practical application at temperature lower than 650 °C, which is usually considered as the preferable operating temperature for SOFC [12]. From the $V-I$ and $P-I$ curves of cells with YSZ electrolyte thin films, it was found that the activation polarization related to the electrode/electrolyte interfaces was the major source for the cell resistance and resulted in low performance of the cells [3,7,8]. In our previous work [3], we demonstrated that microstructure modification of the anode–electrolyte interface could improve the cell performance remarkably by introducing a transition layer consisted of fine NiO/YSZ particles into the interface between anode support and YSZ layer, and the peak power density of a cell with 10- μm thick YSZ electrolyte rose from 407 up to 837 mW cm^{-2} at 800 °C. However, the cell power density decrease rapidly with the temperature, about 214 and 120 mW cm^{-2} at 650 and 600 °C, respectively [3]. A close observation of the $V-I$ curves suggests that there still exists obvious interface polarization. This might be resulted from the cathode–electrolyte interface. In the present work, a function layer of samaria doped ceria (SDC) was applied to the cathode/electrolyte interface, and thus the cell had five layers: NiO/YSZ porous anode support, NiO/YSZ transition layer, YSZ thin film, SDC function layer and $(\text{Pr}_{0.5}\text{Nd}_{0.5})_{0.7}\text{Sr}_{0.3}\text{MnO}_3$ (PNSM)–SDC cathode membrane. The effect of SDC function layer on the cell performance was investigated and the characteristics of the cell with such structure are studied.

2. Experimental

2.1. Powder synthesis

The fine NiO/YSZ and SDC powders used as transition/function layer in this work were prepared by a chemical co-precipitation process with using corresponding metal nitrate as starting precursors and ammonium carbonate as the precipitator. After washing and drying, the resultant powders were subsequently calcined at 950 °C for 2 h.

$(\text{Pr}_{0.5}\text{Nd}_{0.5})_{0.7}\text{Sr}_{0.3}\text{MnO}_3$ and SDC powders used as cathode were synthesized by the glycine–nitrate process (GNP) described in a previous study [13].

2.2. Preparation of NiO/YSZ anode supports

Commercial NiO and YSZ powders of 6:4 in weight ratio was ball milled in ethanol medium for 24 h and dried subsequently, and starch of 20 wt% was added as pore formers. Pellet specimens were made by uniaxially pressing the mixed powders under a pressure of 250 MPa and then pre-calcined at 950 °C for 2 h in air.

2.3. Fabrication of NiO/YSZ transition layer, YSZ thin film and SDC function layer

A suspension with fine NiO/YSZ particle was drop-coated onto the prepared anode support to form a transition layer to modify the surface roughness and the pore size of anode support. YSZ suspension was coated subsequently by the same process onto the transition layer after it being dried in air at room temperature. The thickness of YSZ films was accurately controlled by the suspension volume. Before cathode deposition, the suspension with fine samaria doped ceria (SDC) particles was drop-coated as above onto YSZ electrolyte surface as a function layer. And then the half cells were co-sintered at 1400 °C for 5 h.

2.4. Preparation of cathode

$(\text{Pr}_{0.5}\text{Nd}_{0.5})_{0.7}\text{Sr}_{0.3}\text{MnO}_3$ has been reported as a promising cathode candidate material recently [14]. In this work PNSM was adopted to constitute a composite cathode with SDC. The preparing process of cathode was similar to the previous studies [14]. The cells with cathode layer were finally sintered at 1000 °C for 2 h.

2.5. Evaluation of cell performance

Single cells were sealed on a steel tube with silver paste [15] and tested at 600 and 650 °C in a home-developed cell testing system with humidified hydrogen (3% H_2O) as fuel and stationary air as oxidant. The voltage and output current of the cells were measured by a digital multi-meter (GDM-8145). ac impedance of the cells was conducted using a two-probe impedance spectroscopy (Chenhua Chi604a, Shanghai) under open circuit conditions in the frequency range of 0.01 Hz–100 kHz with 10 mV as the excitation ac amplitude. The microstructure and the morphology of the tested cells were detected using scanning electron microscopy (SEM, model XT30 ESEM-TMP).

3. Results and discussion

A single cell of PEN structure, noted as cell I, was fabricated with NiO/YSZ as anode, YSZ as electrolyte and PNSM/SDC as cathode. The YSZ thin film was formed on porous NiO/YSZ porous support by drop coating, and PNSM/SDC cathode was prepared by suspension spray process. Fig. 1 presents the surface and cross-sectional view of YSZ thin film. It can be seen that the YSZ film about 20 μm was dense, homogeneous and crack free, with only a few small closed pores observed, showing that the drop coating process is an effective technique to fabricate dense YSZ thin membranes on porous ceramic supports.

The current–voltage ($I-V$) and current–power density ($I-P$) of cell I is presented in Fig. 2. With humidified H_2 as fuel, the open circuit voltage (OCV) of the cell is 1.04 V at 600 °C and 1.02 V at 650 °C, respectively. The OCV values are close to the theoretical values predicted by the Nernst equation, indicating that the YSZ electrolyte membrane was dense and there is no gas leakage. The peak power densities of cell I are 100 and

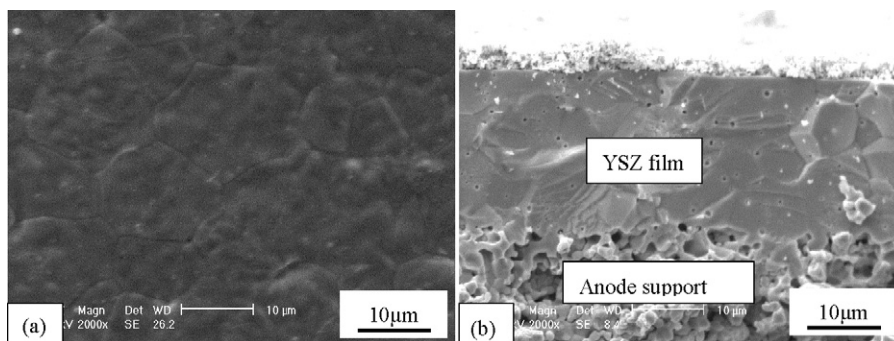


Fig. 1. SEM micrographs of the electrolyte films without transition layer: (a) surface and (b) cross-section.

227 mW cm^{-2} at 600 and 650 °C, respectively, similar to the performance of the cell reported by Xu et al. [8] with NiO/SDC anode, a 10- μm thick YSZ electrolyte and YSB/Ag cathode, of which the peak densities were about 85 and 220 mW cm^{-2} at 600 and 650 °C, respectively. The good performance of cell I indicates that cell I is well assembled. But the performance of cell I is still too low to meet the requirement of commercialization. It can be seen that the I - V curves in Fig. 2 are slightly bending up at low current density. By sectional fitting, the cell resistance at 600 °C is about 4.42 Ωcm^2 at low current density, while 1.58 Ωcm^2 at high current density, indicating that there is obvious activation polarization. The activation polarization is deemed to be resulted from the electrode reaction along with the electrochemical mass transfer at the interfaces between electrolyte and electrodes, which is determined by the electro-catalysis activity of the electrode materials and interface microstructure and so on [16]. That is to say, the bad interfacial connection between electrode and electrolyte could reduce the triple phase boundaries (TPBs), where the electrochemical reaction took place, and thus results in large activation polarization. Shown in Fig. 1b, some large pores appeared at the anode/electrolyte interface (shown in Fig. 1b), which might be the source of large activation polarization.

To ameliorate the anode/electrolyte interfacial condition, a transition layer consisted of fine NiO/YSZ powders was introduced to improve the surface smoothness of the anode support.

The cell with anode transition layer is noted as cell II, and its fracture morphology is presented in Fig. 3. Apparently, an even NiO/YSZ transition layer was obtained, with no big pores at the interface, and a 10- μm thick YSZ film with enhanced interface coherency to the anode support. The peak power densities of cell II are 144 and 353 mW cm^{-2} at 600 and 650 °C, respectively, about 44% and 56% increased with the performance of cell I, as seen from Fig. 4. These values are obviously higher than the values obtained by Yan et al. [3]. However, the activation polarization still exists in the cell with anode transition layer, as seen

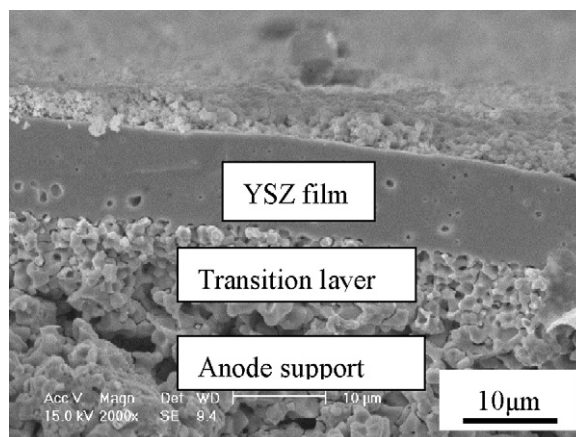


Fig. 3. SEM micrograph of the cell with NiO/YSZ transition layer.

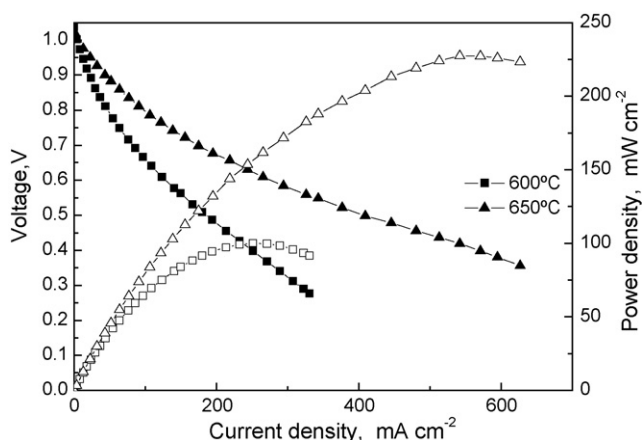


Fig. 2. Voltage and power density for the cell without transition layer measured at 600 and 650 °C.

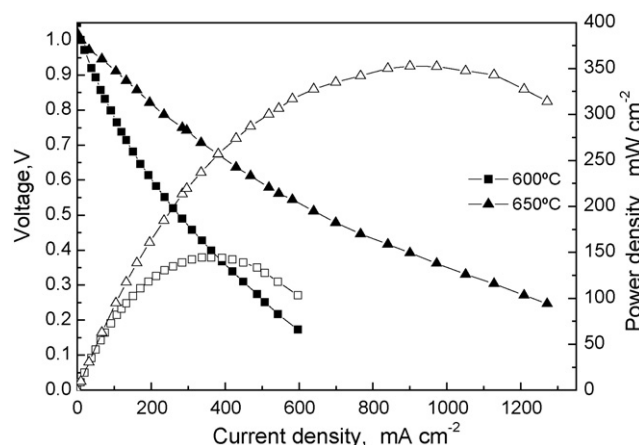


Fig. 4. Voltage and power density for the cell with an anode transition layer measured at 600 and 650 °C.

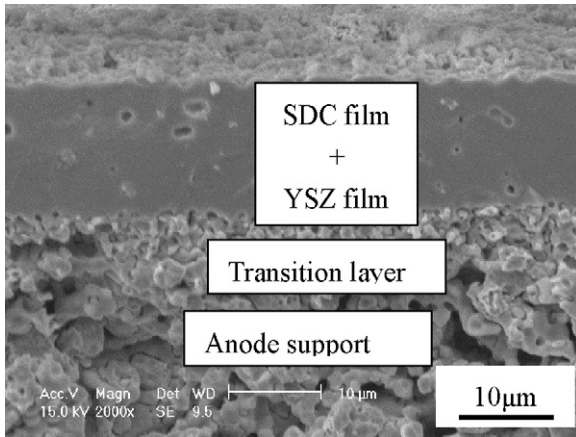


Fig. 5. SEM micrograph of the cell with both NiO/YSZ transition layer and SDC function layer.

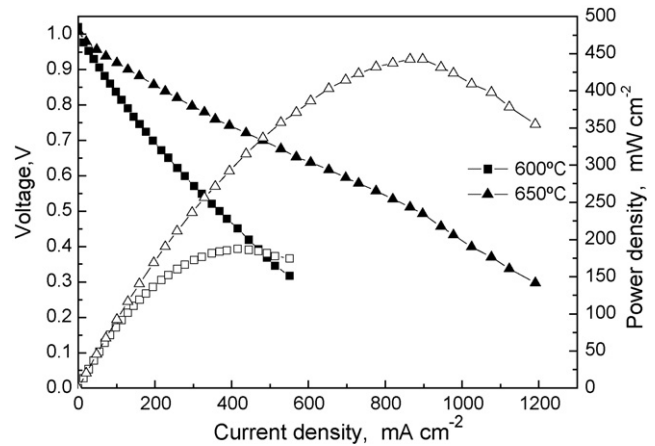


Fig. 6. I - V and I - P characteristics of the cell with both anode transition layer and SDC layer at 600 and 650 °C.

from the I - V curves in Fig. 4. And the cell resistance at low and high current density is calculated as 2.42 and 0.99 Ω cm² at 600 °C, much lower than that of cell I. But there is still a gap between the resistance at low and high current density, which might be attributed to a sluggish electrochemical mass transfer at the cathode–electrolyte interface, as some defects such as big pores and cracks were present.

To enhance the adhesion and the chemical combination between the cathode and the electrolyte, a SDC function layer was introduced between the YSZ electrolyte and the PNSM/SDC cathode. Thus the cell, noted as cell III, is made up of five layers, porous Ni/YSZ anode, Ni/YSZ transition layer, YSZ electrolyte, SDC function layer and PNSM/SDC cathode. Fig. 5 presents the SEM image of cell III. And it can be seen that the SDC layer shows a good combination with YSZ, and even hard to distinguish the interface between YSZ and SDC. More-

over, the cathode adheres well to electrolyte with an ambiguity interface.

Fig. 6 presents I - V and I - P characteristics of cell III using humidified H₂ as fuel and air as oxidant. Peak power densities of the cell at 600 and 650 °C are 187 and 443 mW cm⁻², respectively, showing an increase about 87% and 95% compared with the performance of cell I, and about 30% and 25% compared with that of cell II. The great improvement of cell performance should be attributed to the SDC layer which provides a good conjunction between YSZ and PNSM/SDC, and thus extends the active reacting area to the bulk of cathode to enhance the electrochemical mass transfer process. The I - V curves of cell III is essentially straight, as seen from Fig. 6, indicating that the activation polarization of electrode almost disappeared in such a cell at low temperatures.

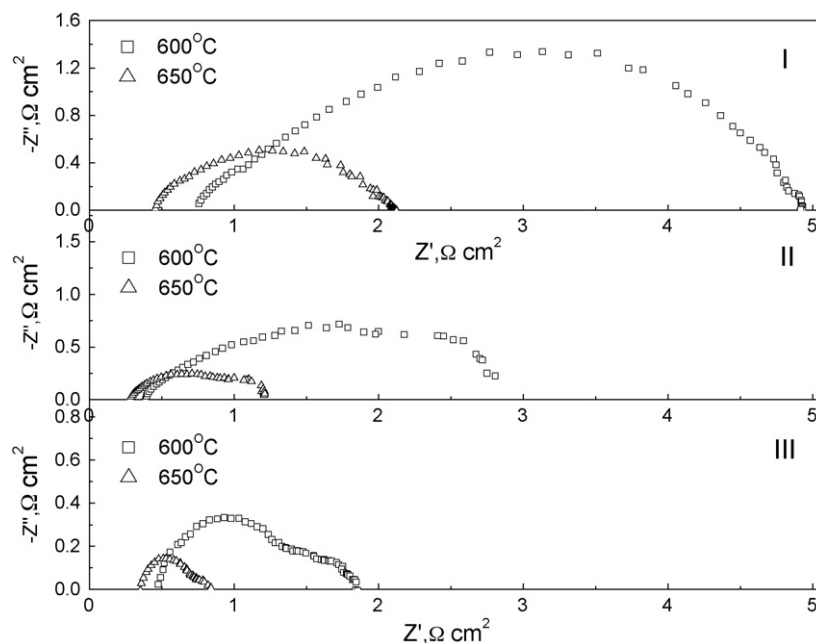


Fig. 7. Impedance spectra of cells: I, with neither transition layer nor function layer; II, with anode transition layer; III with both anode transition layer and SDC function layer at 600 and 650 °C under open circuit voltage.

Table 1
Summarization of the performance of the three cells at 600 and 650 °C

	Temperature (°C)					
	600			650		
	Cell I	Cell II	Cell III	Cell I	Cell II	Cell III
Peak power density (mW cm ⁻²)	100	144	187	227	353	443
Ohmic resistances, R _o (Ω cm ²)	0.76	0.39	0.48	0.46	0.28	0.35
Electrode polarization resistance, R _p (Ω cm ²)	4.16	2.41	1.36	1.66	0.93	0.49
Sectional fitting of the resistance at low current density	4.42	2.42	1.60	1.99	0.94	0.72
Sectional fitting of the resistance at high current density	1.58	0.99	1.05	0.63	0.39	0.48
Decrease of electrode polarization resistance (%)	–	42	67	–	32	64
The ratio of R _p vs. total resistance (%)	85	86	74	78	77	58

Cell I, without transition layer; cell II, with anode transition layer; cell III, with both anode transition layer and SDC function layer.

To intensively investigate the electrochemical characteristics of above cells, ac impedance spectra were also carried out under open-current conditions at different temperatures, as shown in Fig. 7. In the spectra, the intercept of the semicircle to real axis at high frequency (low Z') relates to the ohmic resistance (R_o) and the intercept at low frequency (high Z') represents the total resistances of the cell, while the difference of the two values corresponds to the sum of the electrode polarization resistance (R_p) mainly from electrode–electrolyte interfaces. Values of R_o and R_p determined from the impedance spectra are listed in Table 1.

As we know, the ohmic resistance (R_o) of cell comes from anode, electrolyte and cathode, and the electrolyte resistance (R_e) usually contributes the major part as electrode materials are of much higher conductivity than electrolyte. With the following equation,

$$R_e = \frac{L}{\sigma} \quad (1)$$

where L and σ are the thickness and conductivity of the electrolyte layer, R_e was calculated as 0.72, 0.36, 0.39 Ω cm² at 600 °C and 0.40, 0.20, 0.22 at 650 °C, for cells I, II and III, respectively. It can be seen that R_e is smaller than R_o, about 5–10% less for cell I, while 28–37% less for the other two cells. The difference between R_e and R_o should result from the electrodes. And the electrolyte is thicker; the ratio of R_e to R_o is larger.

The electrode polarization resistance R_p is dominant in the total resistance for all three cells, as shown in Table 1. R_p of cells II and III decreased about 42%, 67% at 600 °C and 32%, 64% at 650 °C, respectively, compared with the values of cell I. The decrease in R_p values and the increase of power densities for cells II and III implies the improved microstructure by interface modification. It should be noted the cell resistances simulated from I – V curves at both high current density and low current density are larger than that from ac impedance spectra. The activation energy for the R_p are roughly calculated to be 123.0, 127.5, 136.7 kJ mol⁻¹, for cells I, II and III, respectively. Similar activation energy for the three cells with different microstructure, suggests that the electrode process mechanisms are similar. To further improve the temperature dependence of the interface resistance, it is necessary to make catalytic modifi-

cation of the interface reaction through using different cathode materials.

4. Conclusions

Severe polarization resistances usually occur in SOFCs with YSZ electrolyte while operated at temperature lower than 800 °C. In this work, a NiO/YSZ transition layer between anode and electrolyte, and a SDC function layer between cathode and electrolyte, were prepared to decrease the activation polarization resulted from the mass transfer at electrode/electrolyte interface. With a NiO/YSZ transition layer, the active polarization simulated from I – V curves drops from 4.42 to 2.42 Ω cm² at 600 °C, about 45% less than that of cell I; with an additional SDC function layer, no activation polarization is obviously observed. The cell performance was remarkably improved with the introduction of both the transition layer and the SDC function layer. Peak power densities of 187 and 443 mW cm⁻² at 600 and 650 °C, respectively, were achieved for a single cell with both a transition layer and a function layer, about ~87% and 95% increased compared with that of the cell without any structural improvement. The study by ac impedance spectroscopy technique indicated that the bulk resistance was mainly related to the thickness of the electrolyte film, while the interfacial polarization resistance which is the main source of cell resistance was effectively reduced by interface improvement. By optimizing the microstructure, it is practical to operate the YSZ-based SOFCs at relatively low temperatures (below 650 °C) in the future.

Acknowledgements

The authors wish to acknowledge funding for this project from specialized research fund for the doctoral program of higher education (20060358034) and National Natural Science Foundation of China (50572099 and 50730002).

References

- [1] S.C. Singhal, K. Kendall (Eds.), High-temperature Solid Oxide Fuel Cells: Fundamentals, Design and Applications, Elsevier, Oxford, UK, 2003.
- [2] H.C. Yu, F. Zhao, A.V. Virkar, K.Z. Fung, J. Power Sources 152 (2005) 22–26.

- [3] R.Q. Yan, D. Ding, B. Lin, M.F. Liu, G.Y. Meng, X.Q. Liu, *J. Power Sources* 164 (2007) 567–571.
- [4] L.P. Meier, L. Urech, L.J. Gauckler, *J. Eur. Ceram. Soc.* 24 (2004) 3753–3758.
- [5] P. Von Dollen, S. Barnett, *J. Am. Ceram. Soc.* 88 (2005) 3361–3368.
- [6] M. Gaudon, C. Laberty-Robert, F. Ansart, P. Stevens, *J. Eur. Ceram. Soc.* 26 (2006) 3153–3160.
- [7] Y.L. Zhang, J.F. Gao, G.Y. Meng, X.Q. Liu, *J. Appl. Electrochem.* 34 (2004) 637–641.
- [8] X.Y. Xu, C.R. Xia, S.G. Huang, D.K. Peng, *Ceram. Int.* 31 (2005) 1061–1064.
- [9] J.M. Wang, Z. Lu, X.Q. Huang, K.F. Chen, N. Ai, J.Y. Hu, W.H. Su, *J. Power Sources* 163 (2007) 957–959.
- [10] G.Y. Meng, C.R. Jiang, J.J. Ma, Q.L. Ma, X.Q. Liu, *J. Power Sources* 173 (2007) 189–193.
- [11] J.W. Kim, A.V. Virkar, K.Z. Fung, K. Mehta, S.C. Singhal, *J. Electrochem. Soc.* 146 (1999) 69–78.
- [12] K. Kuroda, I. Hashimoto, K. Adachi, J. Akikusa, Y. Tamou, N. Komada, T. Ishihara, Y. Takita, *Solid State Ionics* 132 (2000) 199–208.
- [13] R.R. Peng, C.R. Xia, Q.X. Fu, G.Y. Meng, D.K. Peng, *Mater. Lett.* 56 (2002) 1043–1047.
- [14] M.F. Liu, D.H. Dong, L. Chen, J.F. Gao, X.Q. Liu, G.Y. Meng, *J. Power Sources* 176 (2008) 107–111.
- [15] C.R. Xia, M.L. Liu, *Solid State Ionics* 144 (2001) 249–255.
- [16] EG&G Technical Services Inc., *Fuel Cell Handbook*, seventh edition, US Department of Energy, Morgantown, WV, 2004.